Regular Article - Theoretical Physics

Topology of Hořava–Lifshitz black holes in different ensembles

Deyou Chen[1,a]**, Yucheng He**[1,b]**, Jun Tao**[2,c]**, Wei Yang**[3,d]

[1] School of Science, Xihua University, Chengdu 610039, China
[2] Center for Theoretical Physics, College of Physics, Sichuan University, Chengdu 610065, China
[3] School of Information Science and Engineering, Chengdu University, Chengdu 610106, China

Abstract In this paper, we study topological numbers for uncharged and charged static black holes obtained in $z = 3$ Hořava–Lifshitz gravity theory in different ensembles, where z measures the degree of anisotropy between space and time. We first calculate the topological numbers for the uncharged black holes by changing the value of the dynamic coupling constant, and find that the black holes with spherical and flat horizons have the same topological number. When the black hole's horizon is hyperbolic, different values of the coupling constant generate different topological numbers, which can be 1, 0 or -1. This shows that the coupling constant plays an important role in the topological classification. Then we study the topological numbers for the charged black holes in different ensembles. The black hole with a spherical horizon has the same topological number in canonical and grand canonical ensembles. When the horizons are flat or hyperbolic, they have different topological numbers in canonical and grand canonical ensembles. Therefore, the topological numbers for the uncharged black holes are parameter dependent, and those for the charged black holes are ensemble dependent.

Contents

1 Introduction

Topological approaches are effective ways for studying physical systems, which ignore the specific structure of the systems and focus on their general characteristics. Defects are important tools for these approaches, as they reveal certain properties of field configurations. Recently, a topological approach has been used to research on the black holes [1]. In this elegant approach, the black hole solutions are treated as defects in the thermodynamic parameter space. Local thermodynamic stability and instability of a black hole are determined by positive and negative winding numbers, respectively. The global characteristic is characterized by a topological number which is sum of the winding numbers for all the black hole branches at an arbitrary temperature. Each black hole is endowed with a topological number, and then black holes can be classified according to the values of the numbers. This approach was based on Duan's ϕ-mapping topological current theory [2,3], and a key point is the construction of a vector field. In [1], they defined the field through the introduction of a generalized free energy. Based on this work, the influences of the cosmological constant, angular momentum parameters, charges, and other parameters on the topological numbers in the different spacetimes have been extensively researched, and many important results have been found [4–35]. In black hole physics, topological approaches are not limited to the study of black hole classification, but are also used to study light rings and shadows, as well as other natures of black holes [36–43].

In this paper, we study topological numbers for uncharged and charged black holes obtained in the theory of $z = 3$

a e-mail: deyouchen@hotmail.com (corresponding author)

b e-mail: heyucheng365@hotmail.com

c e-mail: taojun@scu.edu.cn

d e-mail: yangweicdu@hotmail.com

Hořava–Lifshitz (HL) gravity in different ensembles. The influence of a dynamical coupling constant for the uncharged black holes and that of different ensembles for the charged black holes on the topological numbers are discussed. HL theory was proposed by Hořava [44–46], which is a non-relativistic renormalizable theory of gravity at a Lifshitz point. At short distances, this theory describes interacting nonrelativistic gravitons. When the condition of detailed balance is restrictively obeyed, it is intimately related to topologically massive gravity in three dimensions. At long distances, it reduces to the relativistic value $z = 1$, where z measures the degree of anisotropy between space and time. Therefore, this theory is seen as a candidate for the UV completion of Einstein's general relativity. Since the theory was proposed, it immediately attracted much attention. Lü first obtained the solutions for spherically symmetric black holes and Friedman–Lemaître–Robertson–Walker cosmology from the HL gravity action [47]. Subsequently, Cai et al. considered a general dynamical coupling constant, and obtained the solution of the topological black holes and discussed their thermodynamic properties [48–50]. The above solutions are for the case of $z = 3$. The black hole solutions of $z = 4$ HL gravity were gotten in [51] and their thermodynamics were studied in [52,53]. Compared with other UV complete gravity theories, HL theory exhibits significantly different UV behaviors. Meanwhile, different values of the coupling constant and different ensembles may affect topological numbers. Therefore, it is necessary to study the topological properties of this theory and the influence of the dynamic coupling constant on topological numbers.

The rest is organized as follows. In the next section, we give a brief review of the topological approach proposed in [1]. In Sect. 3, we study the influence of different values of the dynamic coupling constant on the topological numbers for the uncharged black holes. In Sect. 4, the influence of different ensembles on the topological numbers for the charged black holes is studied. The last section is devoted to our conclusion and discussion.

2 Review of topological approach

In [1], the generalized free energy is defined by

$$\mathcal{F} = E - \frac{S}{\tau}, \tag{2.1}$$

where E and S are the energy and entropy of a system, respectively. τ is a variable and can be seen as the inverse temperature of the cavity enclosing the black hole. This free energy is off-shell except at $\tau = 1/T$. An important vector is constructed via a thermodynamic approach,

$$\phi = \left(\frac{\partial \mathcal{F}}{\partial r_h}, - \cot \Theta \csc \Theta \right). \tag{2.2}$$

where $0 < r_h < +\infty$ and $0 \leq \Theta \leq \pi$. Zero points of the vector obtained at $\tau = 1/T$ and $\Theta = \pi/2$ correspond to the on-shell black hole solution. Other points are not the solutions of Einstein field equations, and then they are the off-shell states. ϕ^Θ diverges at $\Theta = 0$ and $\Theta = \pi$, which leads to that the direction of the vector is outward.

Using Duan's ϕ-mapping topological current theory, one can define a topological current [2,3]

$$j^\mu = \frac{1}{2\pi} \varepsilon^{\mu\nu\rho} \varepsilon_{ab} \partial_\nu n^a \partial_\rho n^b, \tag{2.3}$$

where $\mu, \nu, \rho = 0, 1, 2$, $a, b = 1, 2$, $\partial_\nu = \frac{\partial}{x^\nu}$ and $x^\nu = (\tau, r_h, \Theta)$. τ is seen as a time parameter of the topological defect, and n^a is a unit vector defined by $\frac{\phi^a}{||\phi||}$ ($a = 1, 2$) with $\phi^a = (\phi^{r_h}, \phi^\Theta)$ and $||\phi||$ is the norm of the vector ϕ. It is easy to prove that current is conserved. Using the Jacobi tensor $\varepsilon^{ab} J^\mu(\frac{\phi}{x}) = \varepsilon^{\mu\nu\rho} \partial_\nu \phi^a \partial_\rho \phi^b$ and two-dimensional Laplacian Green function $\Delta_{\phi^a} ln||\phi|| = 2\pi \delta^2(\phi)$, the current is rewritten as [40]

$$j^\mu = \delta^2(\phi) j^\mu \left(\frac{\phi}{x} \right), \tag{2.4}$$

which is nonzero only when $\phi^a(x^i) = 0$. Then a topological number in a parameter region $\sum$ is obtained as follows

$$W = \int_{\sum} j^0 d^2 x = \sum_{i=1}^{N} \beta_i \eta_i = \sum_{i=1}^{N} w_i, \tag{2.5}$$

where $j^0 = \sum_{i=1}^{N} \beta_i \eta_i \delta^2(\vec{x} - \vec{z}_i)$ is the density of the current, β_i is Hopf index which counts the number of the loops that ϕ^a makes in the vector ϕ space when x^μ goes around the zero point z_i. Clearly, this index is always positive. $\eta_i = \text{sign} J^0(\phi/x)_{z_i} = \pm 1$ is the Brouwer degree. w_i is the winding number for the i-th zero point of the vector in the region and its values is independent on the shape of the region.

3 Topological numbers for uncharged HL black holes

The action of the $z = 3$ Horava–Lifshitz theory is written as [44,45]

$$I = \int dt d^3 x (\mathcal{L}_0 + \mathcal{L}_1),$$

$$\mathcal{L}_0 = \sqrt{g} N \left[\frac{2}{\kappa^2} (K_{ij} K^{ij} - \lambda K^2) + \frac{\kappa^2 \mu^2 (\Lambda R - 3\Lambda^2)}{8(1 - 3\lambda)} \right],$$

$$\mathcal{L}_1 = \sqrt{g} N \left[\frac{\kappa^2 \mu^2 (1 - 4\lambda)}{32(1 - 3\lambda)} R^2 \right.$$

$$\left. - \frac{\kappa^2}{2\omega^4} \left(C_{ij} - \frac{\mu\omega^2 R_{ij}}{2} \right) \left(C^{ij} - \frac{\mu\omega^2 R^{ij}}{2} \right) \right], \tag{3.1}$$

where κ^2, λ, μ, ω and Λ are constant parameters, and the Cotten tensor, C_{ij}, is defined by

$$C_{ij} = \epsilon^{ikl} \Delta_k \left(R_l^i - \frac{1}{4} R \delta_l^i \right). \tag{3.2}$$

Comparing the action to that of general relativity, one can get the speed of light, Newton's constant and the cosmological constant,

$$c = \frac{\kappa^2 \mu}{4} \sqrt{\frac{\Lambda}{1 - 3\lambda}}, \quad G = \frac{\kappa^2}{32\pi c}, \quad \Lambda_C = \frac{3}{2}\Lambda. \tag{3.3}$$

$\mathcal{L}_0$ is equivalent to the usual Einstein-Hilbert Lagrangian when $\lambda = 1$. In the HL theory, λ is the dynamical coupling constant, susceptible to quantum corrections [44]. The cosmological constant is negative when $\lambda > 1/3$, and is positive when $\lambda < 1/3$. In this paper, we only consider the negative cosmological constant.

Cai et al. considered a general dynamical coupling constant λ, and obtained the solution of the topological black holes in the HL gravity [48,49]. The metric is

$$ds^2 = -N^2(r)f(r)dt^2 + \frac{dr^2}{f(r)} + r^2 d\Omega_k^2, \tag{3.4}$$

where $d\Omega_k^2$ is the line element for two-dimensional space with constant scalar curvature $2k$. Without loss of generality, we take $k = 1, 0$ and -1 which implies the spherical, flat and hyperbolic horizons, respectively. The functions $f(r)$ and $N(r)$ are given by

$$f(r) = k - \Lambda r^2 - \alpha r^s, \quad N(r) = \gamma r^{1-2s}, \tag{3.5}$$

where α and γ are both integration constants, and s is defined by $s = \frac{2\lambda \pm \sqrt{2(3\lambda-1)}}{\lambda-1}$. In [50], the authors studied the thermodynamical properties of the charged and uncharged topological black holes, and found some interesting result which were never observed in Einstein gravity. The cosmological constant was seen as a fixed constant in the past. Recently, it has been regarded as a variable related to pressure, $P = -\frac{\Lambda}{8\pi} = \frac{3}{8\pi l^2}$, and its conjugate quantity is a thermodynamic volume V. In this paper, we use the initial expression of the cosmological constant. The mass, Hawking temperature, entropy are [48]

$$M = \frac{\sqrt{2}\kappa^2 \mu^2 \Omega_k \gamma}{16\sqrt{3\lambda - 1}} \frac{(k - \Lambda r_h)^2}{r_h^{2s}},$$

$$T = \frac{\gamma}{4\pi r_h^{2s}}[-\Lambda r_h^2(2 - s) - ks],$$

$$S = \frac{\pi \kappa^2 \mu^2 \Omega_k}{\sqrt{2(3\lambda - 1)}} \left[k \ln(\sqrt{-\Lambda}r_h) + \frac{1}{2}(\sqrt{-\Lambda}r_h)^2 \right] + S_0. \tag{3.6}$$

In the above equations, r_h is the horizon radius and S_0 is a constant. When the speed of light $c = \frac{\kappa^2 \mu}{4}\sqrt{\frac{\Lambda}{1-3\lambda}} =$

$\frac{2-s}{1+s}\frac{\kappa^2 \mu \sqrt{-\Lambda}}{4\sqrt{2}}$ and Newton's constant are adopted, the mass and entropy are rewritten as follows [50]

$$M = \frac{c^3 \gamma \Omega_k \Lambda}{16\pi G} \frac{1+s}{s-2} \left(k - \Lambda r_h^2 \right)^2 r_h^{-2s},$$

$$S = \frac{c^3 \Omega_k \Lambda}{4G} \frac{1+s}{s-2}[k \ln(-\Lambda r_h^2) - \Lambda r_h^2] + S_0. \tag{3.7}$$

To study the topological properties, we adopt the definition of the generalized free energy and get

$$\mathcal{F} = \frac{c^3 \gamma \Omega_k \Lambda}{16\pi G r_h^{2s}} \frac{1+s}{s-2} \left(k - \Lambda r_h^2 \right)^2$$

$$- \frac{c^3 \Omega_k \Lambda[k \ln(-\Lambda r_h^2) - \Lambda r_h^2]\frac{1+s}{s-2} + 4GS_0}{4G\tau}. \tag{3.8}$$

We calculate the vector ϕ and obtain its components,

$$\phi^{r_h} = \frac{c^3 \gamma \Omega_k \Lambda \left(k - \Lambda r_h^2 \right)}{8\pi G r_h^{2s+1}} \frac{1+s}{2-s} \left[2\Lambda + s \left(k - \Lambda r_h^2 \right) \right]$$

$$- \frac{c^3 \Omega_k \Lambda}{4G\tau r_h} \frac{1+s}{s-2} \left(k - \Lambda r_h^2 \right),$$

$$\phi^\Theta = -\cot \Theta \csc \Theta. \tag{3.9}$$

Zero points of ϕ^{r_h} determine the topological properties. Let $\phi^{r_h} = 0$ and get the relation between r_h and τ,

$$\tau = -\frac{2\pi r_h^{2s}}{\gamma \left[-2\Lambda r_h^2 - s(k - \Lambda r_h^2) \right]}, \tag{3.10}$$

which shows the change of the inverse temperature with the horizon radius. To clearly and intuitively study the local and global properties of the black holes, we use Eqs. (3.9) and (3.10) and plot Figs. 1, 2, 3, 4, 5, 6 and 7. The influence of the dynamical coupling constant λ on the topological numbers is inversed in these figures. During the calculation, $c = G = \Omega_k = 1$, and r_0 is the length scale of the cavity surrounding the black holes.

From the left picture of Fig. 1, we find that the horizon radius decreases monotonically with the increase of τ's value, which implies that there is only one on-shell black hole solution for an fixed τ's value and no phase transition to appear. Thus the black hole is stable for any temperature. We use the method developed in [1] and find that the winding number is $w = 1$. We order $\tau/r_0 = 50.00$ and plot the picture of the unit vector field in the right picture of the figure. There is one zero point which is at $(r_h/r_0, \Theta) = (21.82, \pi/2)$ in the picture. The winding number can also be calculated by using the method in [40,41], and it is independent of loops that surround the zero point. Thus we calculate it through the red contour $C1$ in Fig. 1. Its winding number is 1, which shows the stability of the black hole. The global characteristic is characterized by the topological number for this black hole, which is $W = w = 1$. In [10], the authors found that the topological number for a four-dimensional Schwarzschild
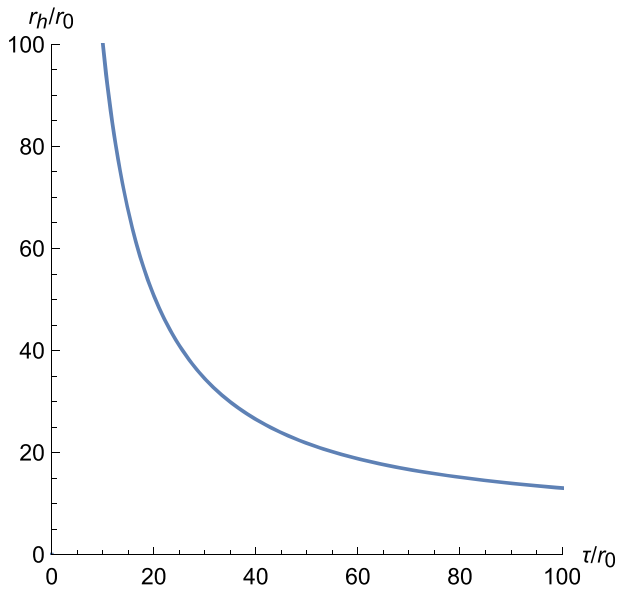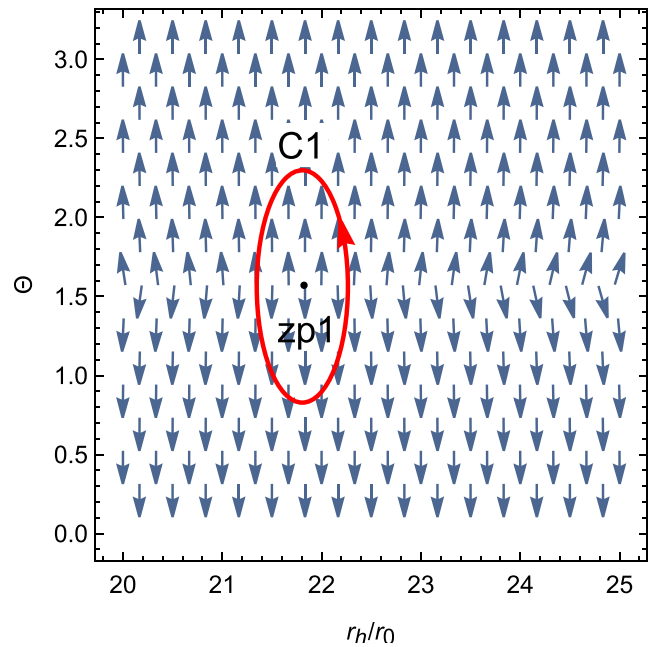
Fig. 1 Topological properties of the uncharged HL black hole, where $k = 1$, $s = 1/2$, $\lambda = 1$, $\gamma = 1$ and $\Lambda r_0^2 = -0.00838$. Zero points of the vector ϕ^{r_h} in the plane $r_h - \tau$ are plotted in the left picture. The unit vector field n on a portion of the plane $\Theta - r_h$ at $\tau/r_0 = 50.00$ is plotted in the right picture. The zero point is at $(r_h/r_0, \Theta) = (21.82, \pi/2)$
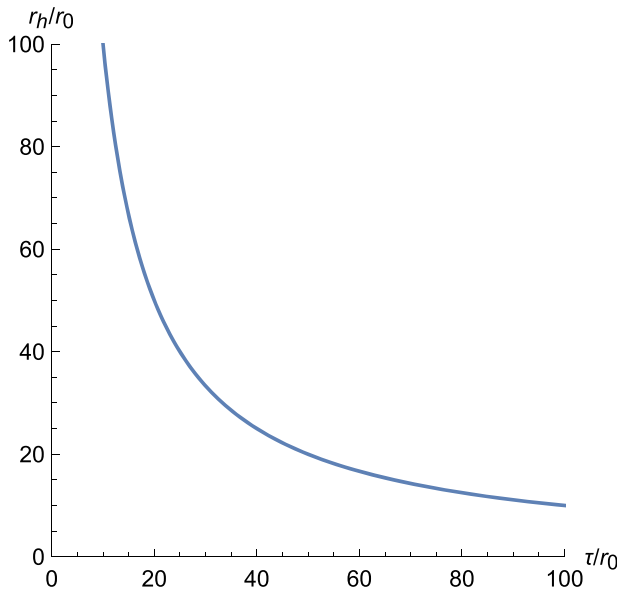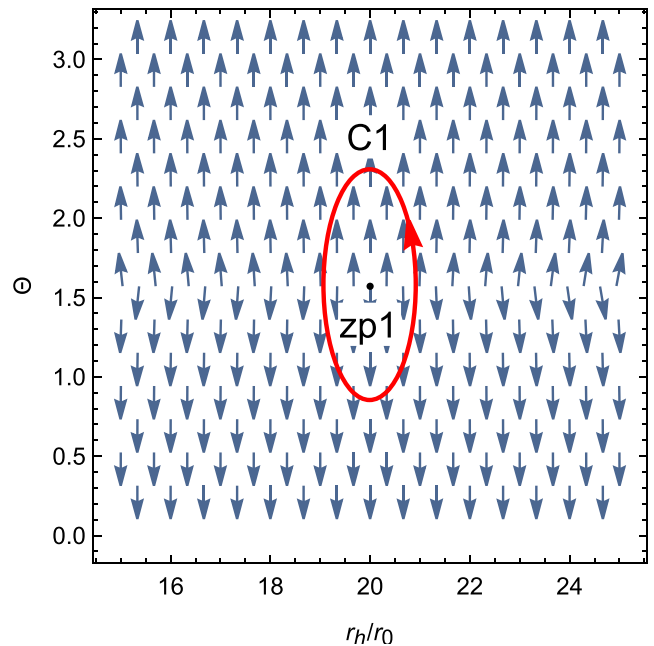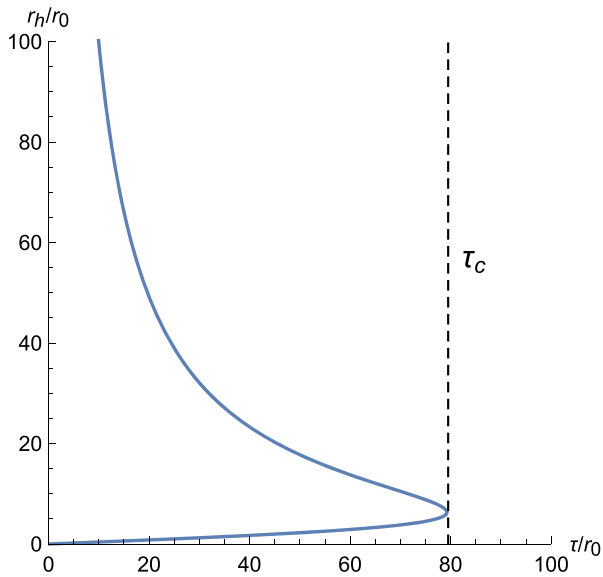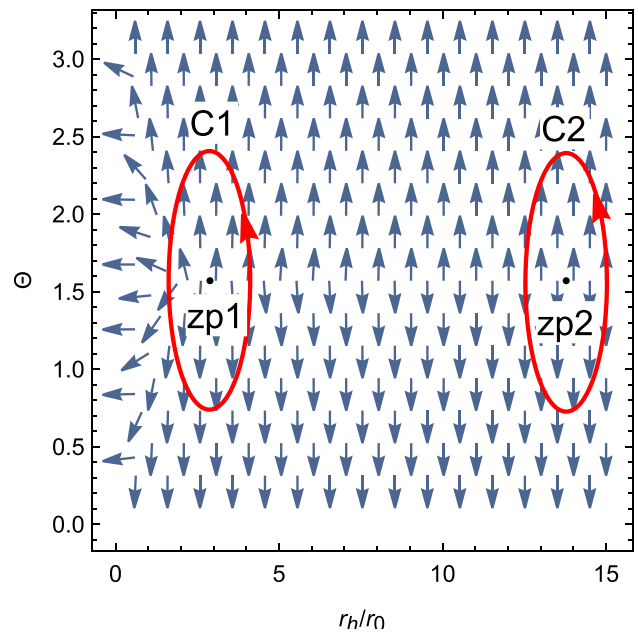

Fig. 2 Topological properties of the uncharged HL black hole, where $k = 0$, $s = 1/2$, $\lambda = 1$, $\gamma = 1$ and $\Lambda r_0^2 = -0.00838$. Zero points of the vector ϕ^{r_h} in the plane $r_h - \tau$ are plotted in the left picture. The unit vector field n on a portion of the plane $\Theta - r_h$ at $\tau/r_0 = 50.00$ is plotted in the right picture. The zero point is at $(r_h/r_0, \Theta) = (20.00, \pi/2)$

Fig. 3 Topological properties of the uncharged HL black hole, where $k = -1$, $s = 1/2$, $\lambda = 1$, $\gamma = 1$ and $\Lambda r_0^2 = -0.00838$. Zero points of the vector ϕ^{r_h} in the plane $r_h - \tau$ are plotted in the left picture. The unit vector field n on a portion of the plane $\Theta - r_h$ at $\tau/r_0 = 60.00$ is plotted in the right picture. Zero points are at $(r_h/r_0, \Theta) = (2.89, \pi/2)$ and $(13.78, \pi/2)$, respectively
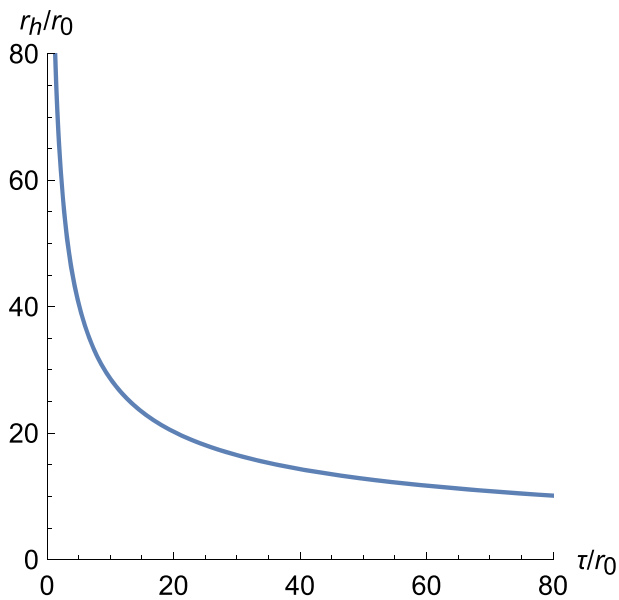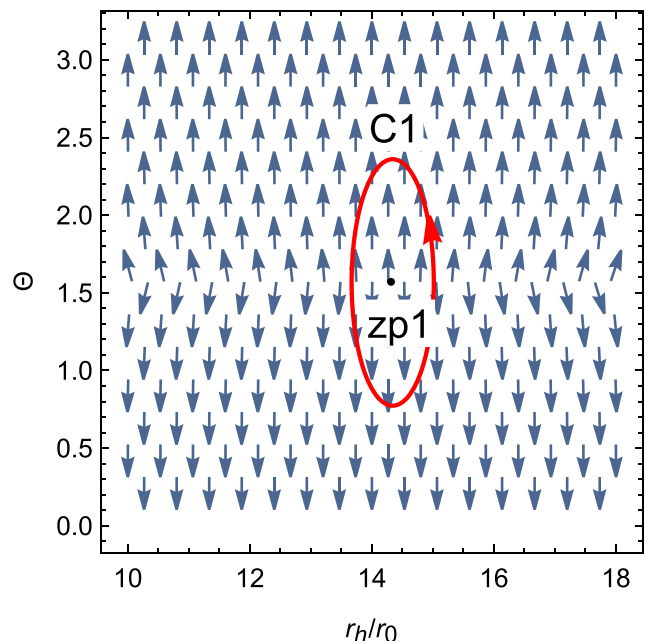

Fig. 4 Topological properties of uncharged HL black holes, where $k = 1$, 0 or -1, $s = 0$, $\lambda = 1/2$ and $\Lambda r_0^2 = -0.00838$. Zero points of the vector ϕ^{r_h} in the plane $r_h - \tau$ are plotted in the left picture. The unit vector field n on a portion of the plane $\Theta - r_h$ at $\tau/r_0 = 40.00$ is plotted in the right picture. The zero point is at $(r_h/r_0, \Theta) = (14.31, \pi/2)$
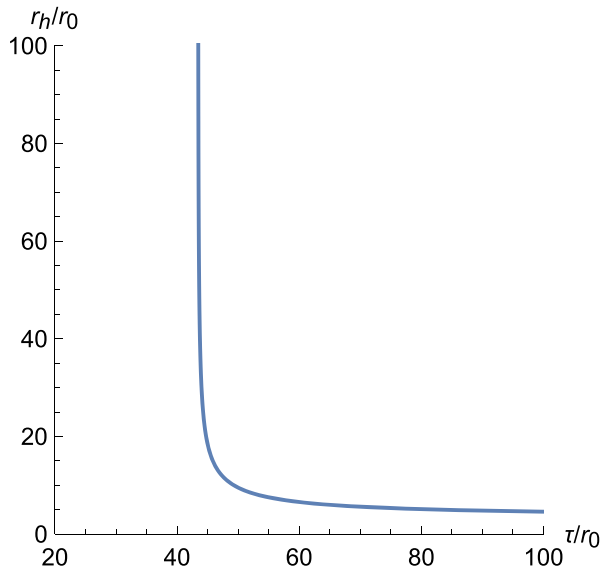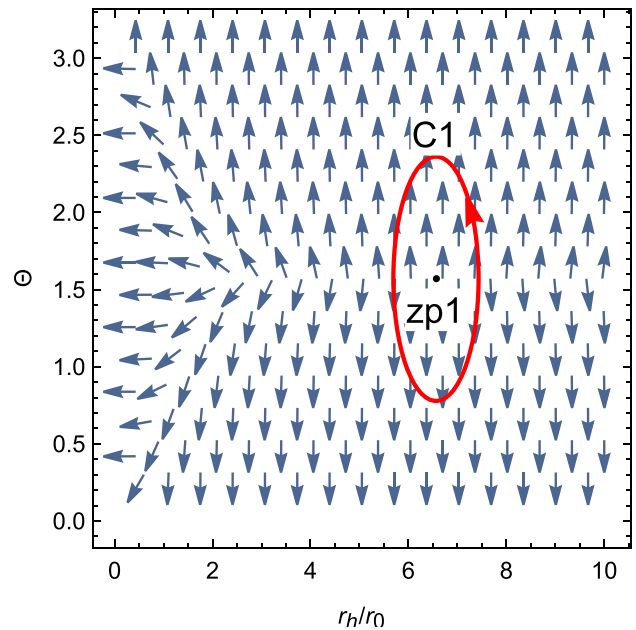
Fig. 5 Topological properties of the uncharged HL black hole, where $k = 1$, $s = 1$, $\lambda = 3$ and $\Lambda r_0^2 = -0.08380$. Zero points of the vector ϕ^{r_h} in the plane $r_h - \tau$ are plotted in the left picture. The unit vector field n on a portion of the plane $\Theta - r_h$ at $\tau/r_0 = 60.00$ is plotted in the right picture. The zero point is at $(r_h/r_0, \Theta) = (6.57, \pi/2)$

AdS black hole is 0. Therefore, this black hole is different from the Schwarzschild AdS black hole in topological class.

When $k = 0$, the horizon is flat and the topological properties are reflected in Fig. 2. It is clearly from the left picture that the topological number is also 1 and there is no phase transition. And then the winding number yielded by the zero point is 1.

When $k = -1$, the metric (3.4) denotes the black hole with a hyperbolic horizon and its topological properties are shown in Fig. 3. There are two on-shell black hole solutions in the left picture. In [1], the authors defined an annihilation point and a generation point based on $\frac{d^2\tau}{dr_h^2} > 0$ and $\frac{d^2\tau}{dr_h^2} < 0$ at a certain point τ_c, respectively. Using these definitions, we find that an annihilation point appears in the left picture of the figure. This annihilation point divides the black hole into a stable region and an unstable region, which yield the winding numbers are 1 and -1, respectively. A second-order phase transition occurs at the annihilation point. There are two horizon radii for a same τ when $\tau < \tau_c = 79.53$, and they coincide with each other at the annihilation point. When $\tau > \tau_c$, there is no black hole existed in the left picture. The positions of the zero points are shown in the right picture of the figure and are located at $(2.89, \pi/2)$ and $(13.78, \pi/2)$, respectively. The winding numbers corresponding to these two points are 1 and -1, respectively. Thus the topological number is 0.

When $\lambda = 1/2$, there is $s = 0$, and it is easy to find from Eq. (3.10) that the value of τ is independent of k. Thus the
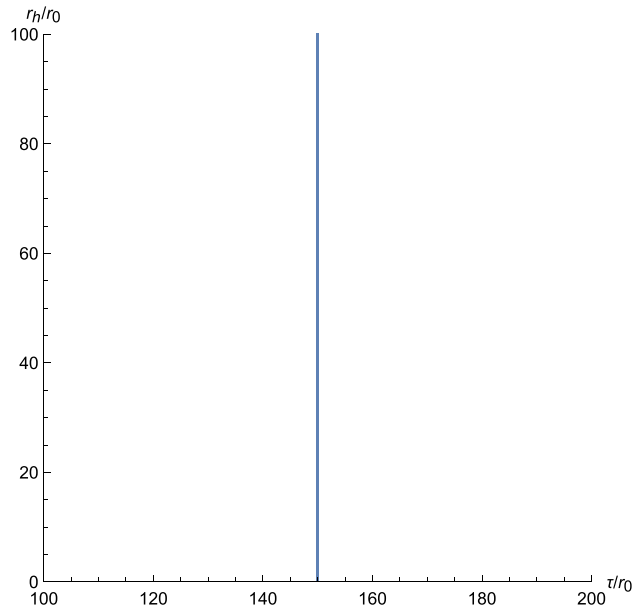

Fig. 6 Zero points of the vector ϕ^{r_h} in the plane $r_h - \tau$, where $k = 0$, $s = 1$, $\lambda = 3$ and $\Lambda r_0^2 = -0.08380$

topological properties of the black holes with the spherical, flat and hyperbolic horizons are shared by Fig. 4. In the figure, the horizon radii decrease monotonically with the increase of τ's value, which shows that the black holes are stable for any temperature and the winding number is 1. The black holes have a same topological number 1. The zero points are
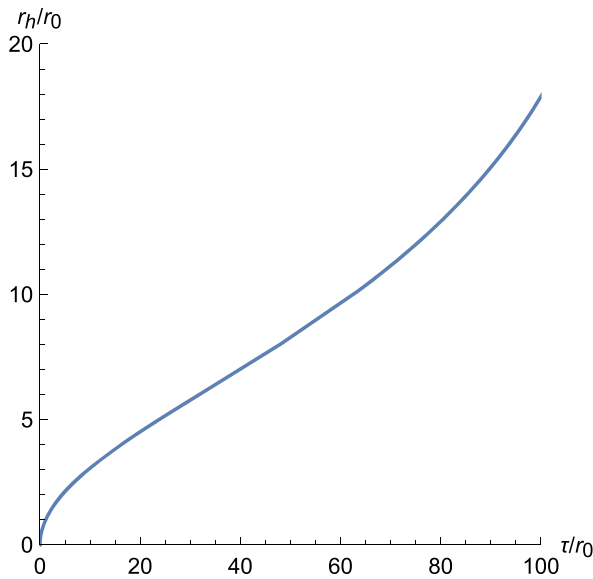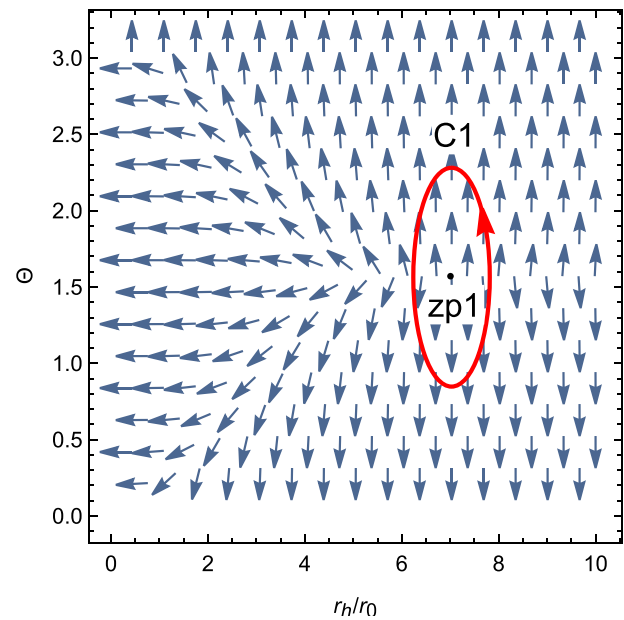
Fig. 7 Topological properties of the uncharged HL black hole, where $k = -1$, $s = 1$, $\lambda = 3$ and $\Lambda r_0^2 = -0.00838$. Zero points of the vector ϕ^{r_h} in the plane $r_h - \tau$ are plotted in the left picture. The unit vector field n on a portion of the plane $\Theta - r_h$ at $\tau/r_0 = 40.00$ is plotted in the right picture. The zero point is at $(r_h/r_0, \Theta) = (7.01, \pi/2)$

located at the same position. This shows that the dynamical coupling constant λ plays an important role in the topological class of the black holes.

When $\lambda = 3$, we get $s = 1$ and plot Figs. 5, 6 and 7. From Fig. 5, we find that when the τ's value decreases at a certain value, the horizon radius increase very fast. The black hole is stable for any τ's value and its winding number is 1. The zero point is at $(r_h/r_0, \Theta) = (6.57, \pi/2)$. Therefore, its topological number is 1.

When $k = 0$, it is easy to find from Eq. (3.10) that the τ's value is independent on the horizon radius. Therefore, the variation of r/r_0 with τ/r_0 is a vertical line parallel to the vertical axis in Fig. 6. The horizon radius is not affected by the τ's value, and the black hole is stable. It is natural to obtain the topological number of 1.

When $k = -1$, Fig. 7 is plotted. In the figure, the horizon radius increase monotonically with the τ's value, which shows that the black hole is unstable for any τ's value and its winding number is -1. The zero point is at $(7.01, \pi/2)$ for $\tau/r_0 = 40.00$ and corresponds to the winding number -1. Therefore, the topological number is -1.

Comparing Figs. 1, 2, 3, 4, 5, 6 and 7, it is evident that the uncharged black hole with the spherical and flat horizons have the same topological number. However, for the different values of λ in the uncharged black hole with the hyperbolic horizon, its topological numbers can be 1, 0 or -1. Therefore, its topological number is parameter dependent.

4 Topological numbers for charged HL black holes in different ensembles

The solution of the charged black hole in the HL gravity theory with an electromagnetic field was gotten when $s = 1/2$ and $\lambda = 1$ [48]. It is also given by the metric (3.4). Now the functions $N(x) = 1$ and $f(x) = k + \frac{x^2}{1-\epsilon^2} - \frac{\sqrt{\epsilon^2 x^4 + (1-\epsilon^2)(c_0 x - q^2/2)}}{1-\epsilon^2}$. Taking the limit $\epsilon \to 1$, the solution becomes $f(x) = k + \frac{x^2}{2} - \frac{c_0}{2x} + \frac{q^2}{4x^2}$, which is the AdS Reissner–Nordström black hole solution. Our interest is focused on the solution with $\epsilon^2 = 0$. Taking $\epsilon^2 = 0$, the function is

$$f(x) = k + x^2 - \sqrt{c_0 x - \frac{q^2}{2}}, \tag{4.1}$$

where $x = \sqrt{-\Lambda} r$, q and c_0 are integral constants. c_0 can be expressed as $c_0 = \frac{2k^2 + q^2 + 4kx_+^2 + 2x_+^4}{2x_+}$, and $x_+ = \sqrt{-\Lambda} r_h$ is determined by $f(x_+) = 0$, where r_h is the horizon radius. The black hole's mass and charge are $M = \frac{\kappa^2 \mu^2 \Omega_k \sqrt{-\Lambda} c_0}{16}$ and $Q = \frac{\kappa^2 \mu^2 \Omega_k \sqrt{-\Lambda} q}{16}$, respectively. We also use speed of light and Newton's constant to rewrite the mass and charge as follows,

$$M = \frac{c^3 \Omega_k c_0}{16\pi G \sqrt{-\Lambda}}, \quad Q = \frac{c^3 \Omega_k q}{16\pi G \sqrt{-\Lambda}}. \tag{4.2}$$
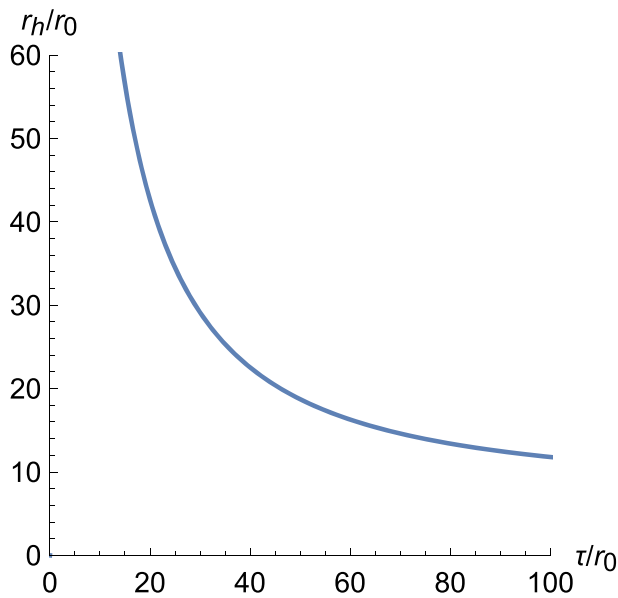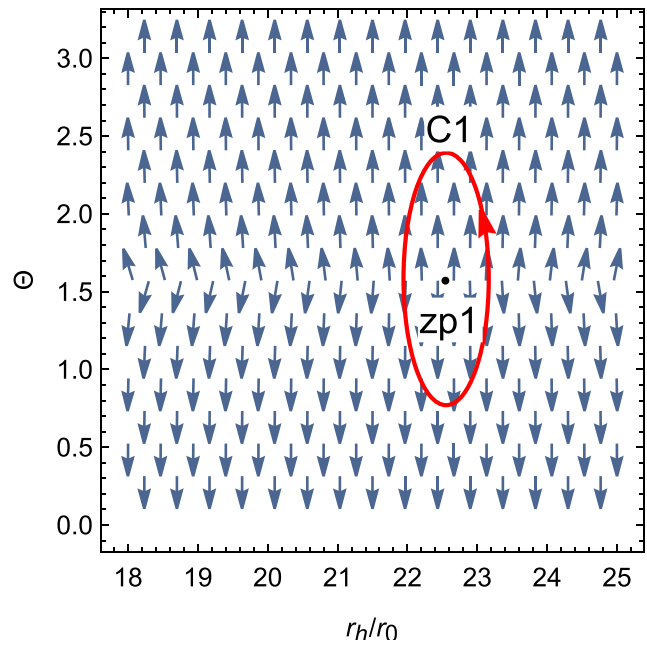
Fig. 8 Topological properties of the charged HL black hole in the canonical ensemble, where $k = 1$ and $\Lambda r_0^2 = -0.01$. Zero points of the vector ϕ^{r_h} in the plane $r_h - \tau$ are plotted in the left picture. The unit vector field n on a portion of the plane $\Theta - r_h$ at $\tau/r_0 = 40.00$ is plotted in the right picture. The zero point is at $(r_h/r_0, \Theta) = (22.54, \pi/2)$

The Hawking temperature, entropy and electromagnetic potential are

$$T = \sqrt{-\Lambda}\frac{6x_+^4 + 4k^2x_+^2 - 2k^2 - q^2}{16\pi kx_+ + 16\pi x_+^3},$$

$$S = -\frac{c^3\Omega_k}{4G\Lambda}\left(2k\ln x_+ + x_+^2\right) + S_0,$$

$$\Phi = \frac{q}{x_+} + \Phi_0, \tag{4.3}$$

respectively, where S_0 and Φ_0 are constants. In the following, we study the topological numbers for this black hole in canonical and grand canonical ensembles, respectively.

4.1 Topological numbers in canonical ensemble

For a canonical ensemble, there is only an exchange of energy between the system and the external environment, and the system's temperature, volume and particle number remain be unchanged. We use the definition of the generalized free energy and get

$$\mathcal{F} = \frac{c^3\Omega_k c_0}{16\pi G\sqrt{-\Lambda}} + \frac{c^3\Omega_k\left(2k\ln x_+ + x_+^2\right) + 4S_0}{4G\Lambda\tau}. \tag{4.4}$$

According to the definition of the vector ϕ, its components are

$$\phi^{r_h} = \frac{c^3\Omega_k\left(2k^2 + q^2 - 4kx_+^2 - 6x_+^4\right)}{32\pi Gx_+^2} - \frac{c^3\Omega_k\left(x_+^2 + k\right)}{2G\tau\sqrt{-\Lambda}x_+},$$

$$\phi^\Theta = -\cot\Theta\csc\Theta. \tag{4.5}$$

We let $\phi^{r_h} = 0$, and get the relation between τ and r_h, which is

$$\tau = \frac{16\pi(x_+^3 + kx_+)}{\sqrt{-\Lambda}(6x_+^4 + 4kx_+^2 - 2k^2 - q^2)}. \tag{4.6}$$

In this section, we also order $c = G = \Omega_k = 1$ and $q = 1$ to plot Figs. 8, 9 and 10 and to describe its topological properties. In the figures, we can get the winding numbers from the change of r_h with τ which reflects the local properties, and the topological numbers which is the sum of the winding numbers.

In Fig. 8, the radius of the event horizon monotonically decreases with the increase of τ's value, which shows that the black hole is stable for any τ's value and there is no phase transition to appear. It is easy to get the winding number as 1. Thus the topological number for the black hole with the spherical horizon is 1. When $\tau/r_0 = 40.00$, the unit vector field n is plotted in the right picture of the figure. There is only one zero point which is at $(22.54, \pi/2)$, which also shows the topological number is 1. In [1], the authors have found that the topological number for the four-dimensional RN AdS black hole is 1, therefore, both this black hole and the RN AdS black hole belong to a class with a topological number of 1.

It is also easy to find from Fig. 9 that the topological number of the black hole with the flat event horizon is 1. The zero point is at $(21.12, \pi/2)$ in this figure.
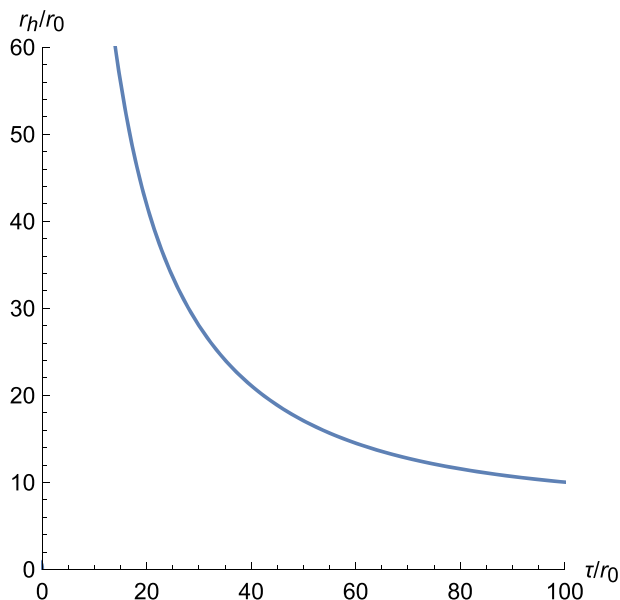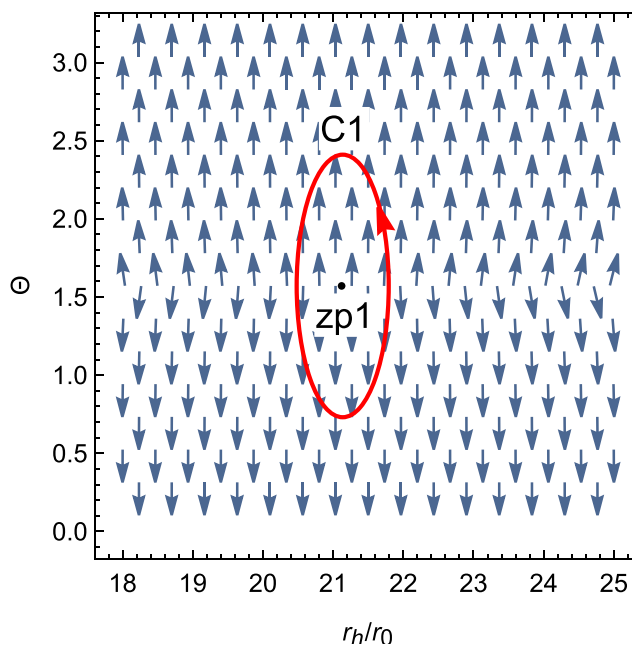
Fig. 9 Topological properties of the charged HL black hole in the canonical ensemble, where $k = 0$ and $\Lambda r_0^2 = -0.01$. Zero points of the vector ϕ^{r_h} in the plane $r_h - \tau$ are plotted in the left picture. The unit vector field n on a portion of the plane $\Theta - r_h$ at $\tau/r_0 = 40.00$ is plotted in the right picture. The zero point is at $(r_h/r_0, \Theta) = (21.12, \pi/2)$

Unlike the previous two figures, there are two curves in Fig. 10. The upper curve represents a monotonic decrease of the horizon radius with the increase of τ's value, which leads to the winding number 1. For another curve, an annihilation point divides the black hole into stable and unstable regions, and their winding numbers are 1 and -1, respectively. We used the approach in [14] to calculate the topological number for the black hole with the hyperbolic horizon by considering the combination effect of these two curves. Therefore, the topological number is 1. In the right picture, the zero points are at $(r_h/r_0, \Theta) = (4.38, \pi/2)$, $(7.30, \pi/2)$ and $(15.38, \pi/2)$, which generate the winding numbers of 1, -1, and 1, respectively. On the other hand, a heat capacity is an effective tool for distinguishing the thermodynamic stability and second-order phase transitions in thermodynamic systems [22]. The heat capacity of this black hole is $C_Q = T \left(\frac{\partial S}{\partial T}\right)_Q = \frac{(k - r_h^2 \Lambda)^2 [q^2 + 2(k - r_h^2 \Lambda)(k + 3 r_h^2 \Lambda)]}{2\Lambda(k - 3 r_h^2 \Lambda)[q^2 + 2(k - r_h^2 \Lambda)^2]}$. We focus our interest on the case of $k = -1$. It is easy to obtain that the heat capacity diverges at $T^{-1} = \tau_c = 52.75$, which implies that the second-order phase transition occurs. The heat capacity is greater than zero at $r_h = 4.34$ and 15.38, which means the stability of the black hole. The heat capacity is less than zero at point $r_h = 7.30$, which indicates the instability of the black hole.

4.2 Topological numbers in grand canonical ensemble

In the grand canonical ensemble, the system can exchange the energy and charge with the outside, and its temperature, volume and chemical potential remain be unchanged. Now the generalized free energy is defined by

$$
\begin{aligned}
\mathcal{F} &= E - Q\Phi - \frac{S}{\tau} \\
&= \frac{c^3 \Omega_k c_0}{16\pi G \sqrt{-\Lambda}} \\
&\quad - \frac{c^3 \Omega_k q}{16\pi G \sqrt{-\Lambda}} \left(\frac{q}{x_+} + \Phi_0\right) \\
&\quad + \frac{c^3 \Omega_k \left(2k \ln x_+ + x_+^2\right) + 4S_0}{4G\Lambda \tau}.
\end{aligned} \tag{4.7}
$$

We use the definition of the vector ϕ, and get its components,

$$
\phi^{r_h} = \frac{c^3 \Omega_k \left(2k^2 - q^2 - 4kx_+^2 - 6x_+^4\right)}{32\pi G x_+^2} - \frac{c^3 \Omega_k \left(x_+^2 + k\right)}{2G\tau \sqrt{-\Lambda} x_+},
$$

$$
\phi^{\Theta} = -\cot\Theta \csc\Theta. \tag{4.8}
$$

Solving $\phi^{r_h} = 0$ yields the relation

$$
\tau = \frac{16\pi \left(x_+^3 + kx_+\right)}{\sqrt{-\Lambda}\left(6x_+^4 + 4kx_+^2 - 2k^2 + q^2\right)}. \tag{4.9}
$$

We use Eqs. (4.8) and (4.9) and plot Figs. 11, 12 and 13 to describe the topological properties. Clearly, the topological
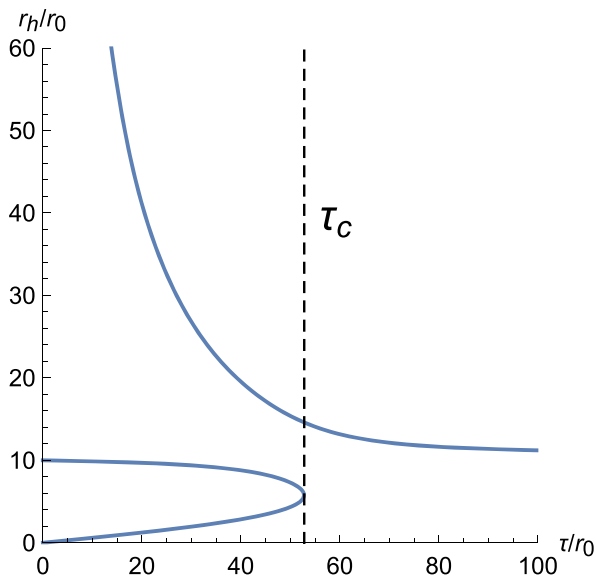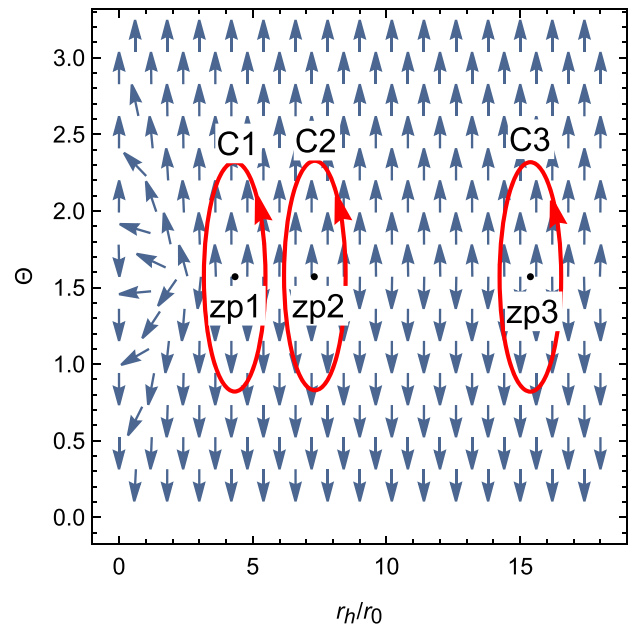
Fig. 10 Topological properties of the charged HL black hole in the canonical ensemble, where $k = -1$ and $\Lambda r_0^2 = -0.01$. Zero points of the vector ϕ^{r_h} in the plane $r_h - \tau$ are plotted in the left picture. The unit vector field n on a portion of the plane $\Theta - r_h$ at $\tau/r_0 = 50.00$ is plotted in the right picture. The zero point is at $(r_h/r_0, \Theta) = (4.34, \pi/2)$, $(7.30, \pi/2)$ and $(15.38, \pi/2)$, respectively
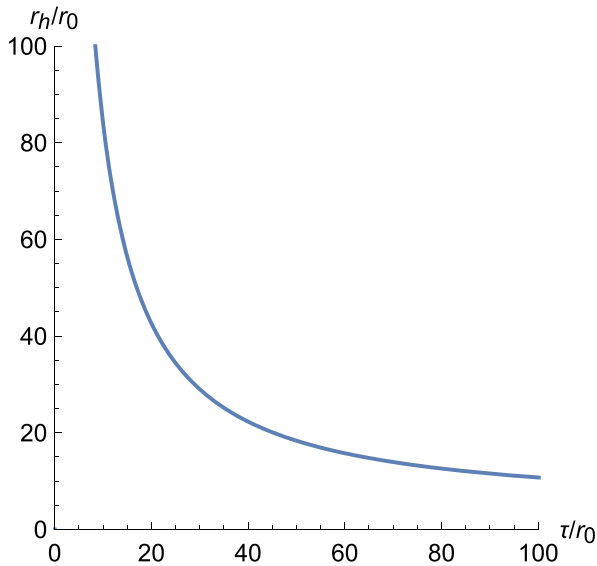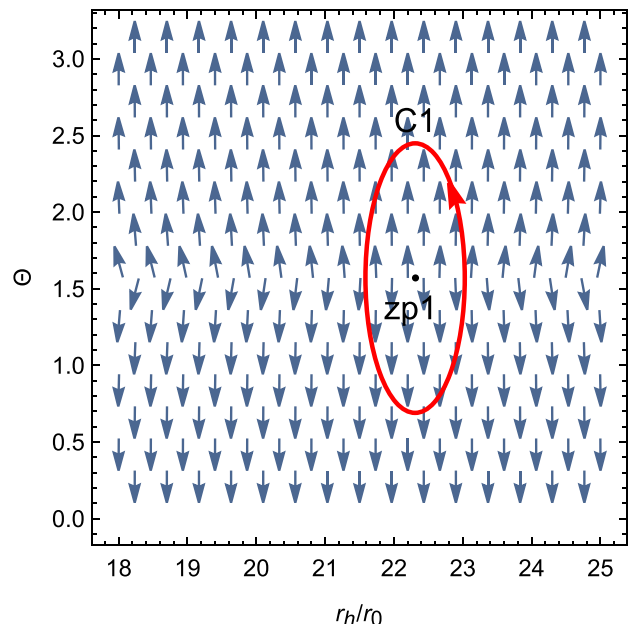

Fig. 11 Topological properties of the charged HL black hole in the grand canonical ensemble, where $k = 1$ and $\Lambda r_0^2 = -0.01$. Zero points of the vector ϕ^{r_h} in the plane $r_h - \tau$ are plotted in the left picture. The unit vector field n on a portion of the plane $\Theta - r_h$ at $\tau/r_0 = 40.00$ is plotted in the right picture. The zero point is at $(r_h/r_0, \Theta) = (22.31, \pi/2)$
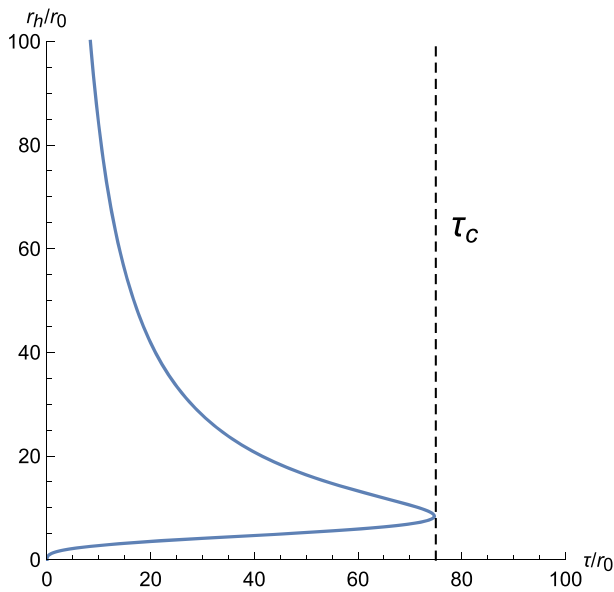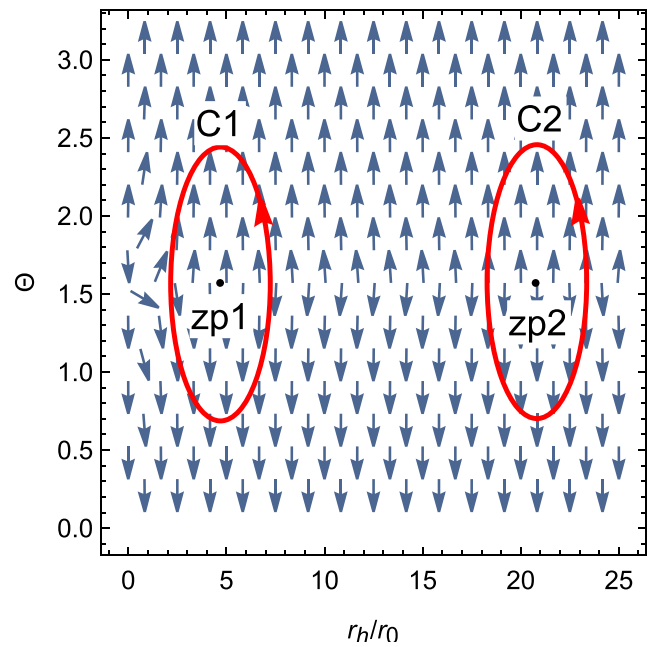
Fig. 12 Topological properties of the charged HL black hole in the grand canonical ensemble, where $k = 0$ and $\Lambda r_0^2 = -0.01$. Zero points of the vector ϕ^{r_h} in the plane $r_h - \tau$ are plotted in the left picture. The unit vector field n on a portion of the plane $\Theta - r_h$ at $\tau/r_0 = 40.00$ is plotted in the right picture. The zero points are at $(r_h/r_0, \Theta) = (4.68, \pi/2)$ and $(20.76, \pi/2)$, respectively
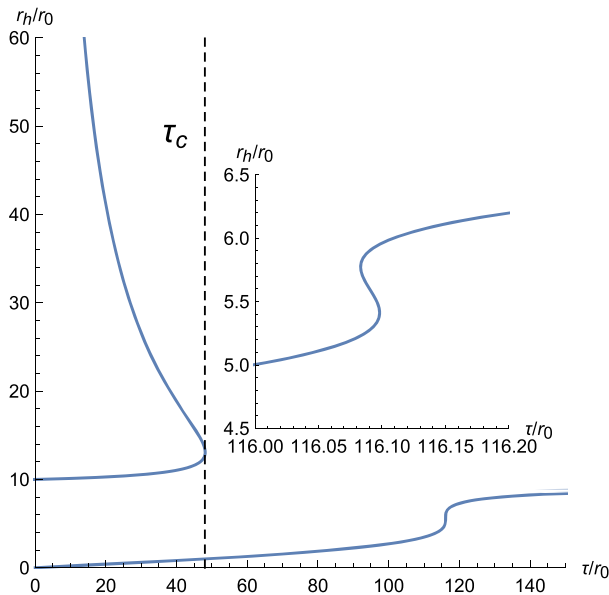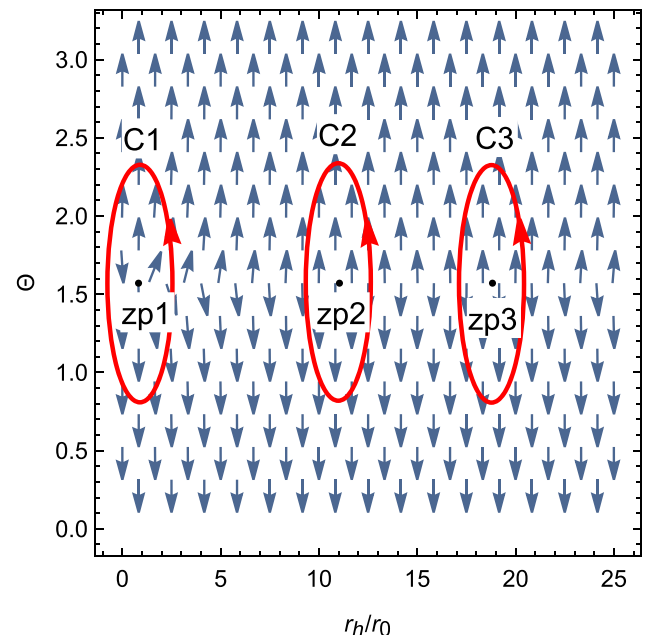

Fig. 13 Topological properties of the charged HL black hole in the grand canonical ensemble, where $k = -1$ and $\Lambda r_0^2 = -0.01$. Zero points of the vector ϕ^{r_h} in the plane $r_h - \tau$ are plotted in the left picture. The unit vector field n on a portion of the plane $\Theta - r_h$ at $\tau/r_0 = 40.00$ is plotted in the right picture. The zero point is at $(r_h/r_0, \Theta) = (0.82, \pi/2)$, $(11.04, \pi/2)$ and $(18.83, \pi/2)$, respectively

number for the black hole with the spherical horizon in Fig. 11 is 1, which is same as that in the canonical ensemble.

In Fig. 12, an annihilation point appears when $\tau_c = 75.09$ and it divides the black hole into the stable and unstable regions. The phase transition occurs at this annihilation point. In the stable region, the horizon radius monotonically decreases with the increases of τ's value. In the unstable region, the horizon radius monotonically increases with the increases of τ's value. Its topological number is 0. The zero points are at $(r_h/r_0, \Theta) = (4.68, \pi/2)$ and $(20.76, \pi/2)$, respectively.

There are two separate curves in Fig. 13. The upper left curve has a stable black hole region and an unstable black hole region, with a winding number of 1 and -1, respectively. The phase transition occurs at the annihilation point $\tau_c = 48.12$. For another curve, a generation point and an annihilation point divide the black hole into three regions. These three regions correspond to a large black hole, an intermediate black hole, and a small black hole, respectively. The winding numbers for them are -1, 1, and -1, respectively. Thus the topological number is -1. It is easy to find from the figure that there is a small-large black hole phase transition near an inverse temperature of $\tau/r_0 = 116.00$. The right picture shows three zero points, which were obtained at $\tau/r_0 = 40.00$. The winding numbers corresponding to these three zeros are -1, 1, and -1, respectively. Therefore, the sum of the three also yields a topological number of -1. It should be noted that when we take $\tau/r_0 = 40.00$, we can only obtain three zero points. When $\tau/r_0 = 116.00$, three other zero points can be obtained, which are not shown in the figure. Considering the winding numbers in both cases, we can also obtain a topological number of -1.

Compared with the results in the canonical ensemble, it is not difficult to find that the black hole with the spherical horizon has the same topological number in the canonical and grand canonical ensembles, while the black holes with the flat and hyperbolic horizons have different topological numbers in the canonical and grand canonical ensembles. Therefore, the topological numbers for the black holes with the flat and hyperbolic horizons are ensemble dependent.

5 Conclusion and discussion

In this work, we studied the topological numbers for the uncharged and charged black holes in the HL gravity. The influence of the dynamical coupling constant λ on the topological numbers for the uncharged black holes has been extensively discussed. For the charged black holes, their topological numbers in the canonical and grand canonical ensembles were studied. The numbers for these black holes obtained in the work are listed in Tables 1 and 2.

Table 1 Topological numbers of uncharged HL black holes. BH is the abbreviation for the HL black hole, and TNs is the abbreviation for the topological numbers

Black hole solutions	TNs
Uncharged BH with the spherical horizon	1
Uncharged BH with the flat horizon	1
Uncharged BH with the hyperbolic horizon	1, 0 or -1

Table 2 Topological numbers of charged HL black holes in different ensembles. CE is the abbreviation for the canonical ensemble, and GCE is the abbreviation for the grand canonical ensemble

Black hole solutions	TNs in CE	TNs in GCE
Charged BH with the spherical horizon	1	1
Charged BH with the flat horizon	1	0
Charged BH with the hyperbolic horizon	1	-1

For the uncharged black holes with the spherical and flat horizons, their topological numbers are the same and independent on the value of the coupling constant. For the uncharged black hole with the hyperbolic horizon, different values of the coupling constant result in different topological numbers, which indicates that the topological number for this black hole is parameter dependent. This coupling constant plays an important role in the topological class of black holes. We have also studied the topological numbers for the charged black holes in the canonical and grand canonical ensembles. In these two ensembles, the topological numbers for the charged black hole with the spherical horizon are the same. While the black holes with the flat and hyperbolic horizons have different topological numbers in these two ensembles. This shows that the last two black holes are ensemble dependent.

On the other hand, according to topological classification, the charged black hole with a spherical horizon and the uncharged black hole belong to the same class because they have the same topological number. Due to the fact that the uncharged and charged black holes with flat and hyperbolic horizons are parameter dependent and ensemble dependent, respectively, it is necessary to consider the parameters' values and ensemble's selection when classifying them. Furthermore, our work is limited to the influence of the dynamic coupling constant on the topological numbers for the static HL black holes. Whether this constant also has an important influence on the number for rotating HL black holes needs to be further confirmed in future work.

References

1. S.W. Wei, Y.X. Liu, R.B. Mann, Black hole solutions as topological thermodynamic defects. Phys. Rev. Lett. **129**, 191101 (2022)
2. Y.S. Duan, M.L. Ge, SU(2) gauge theory and electrodynamics of N moving magnetic monopoles. Sci. Sin. **9**, 1072 (1979)
3. Y.S. Duan, The structure of the topological current, SLAC-PUB-3301 (1984)
4. N.C. Bai, L. Li, J. Tao, Topology of black hole thermodynamics in Lovelock gravity. Phys. Rev. D **107**, 064015 (2023)
5. P.K. Yerra, C. Bhamidipati, S. Mukherji, Topology of critical points and Hawking–Page transition. Phys. Rev. D **106**, 064059 (2022)
6. P.K. Yerra, C. Bhamidipati, Topology of black hole thermodynamics in Gauss–Bonnet gravity. Phys. Rev. D **105**, 104053 (2022)
7. P.K. Yerra, C. Bhamidipati, Topology of Born–Infeld AdS black holes in 4D novel Einstein–Gauss–Bonnet gravity. Phys. Lett. B **835**, 137591 (2022)
8. P.K. Yerra, C. Bhamidipati, S. Mukherji, Topology of critical points in boundary matrix duals. arXiv:2304.14988 [hep-th]
9. D. Wu, Topological classes of rotating black holes. Phys. Rev. D **107**, 024024 (2023)
10. D. Wu, S.Q. Wu, Topological classes of thermodynamics of rotating AdS black holes. Phys. Rev. D **107**, 084002 (2023)
11. D. Wu, Classifying topology of consistent thermodynamics of the four-dimensional neutral Lorentzian NUT-charged spacetimes. Eur. Phys. J. C **83**, 365 (2023)
12. D. Wu, Topological classes of thermodynamics of the four-dimensional static accelerating black holes. Phys. Rev. D **108**, 084041 (2023)
13. D. Wu, Consistent thermodynamics and topological classes for the four-dimensional Lorentzian charged Taub-NUT spacetimes. Eur. Phys. J. C **83**, 589 (2023)
14. D. Wu, Topological classes of thermodynamics of the four-dimensional static accelerating black holes. Phys. Rev. D **108**, 084041 (2023)
15. C. Liu, J. Wang, Topological natures of the Gauss-Bonnet black hole in AdS space. Phys. Rev. D **107**, 064023 (2023)
16. Z.Y. Fan, Topological interpretation for phase transitions of black holes. Phys. Rev. D **107**, 044026 (2023)
17. Y.B. Du, X.D. Zhang, Topological classes of BTZ black holes. arXiv:2302.11189 [gr-qc]
18. Y.B. Du, X.D. Zhang, Topological classes of black holes in de-Sitter spacetime. Eur. Phys. J. C **83**, 927 (2023)
19. M. Zhang, J. Jiang, Bulk-boundary thermodynamic equivalence: a topology viewpoint. JHEP **2306**, 115 (2023)
20. C.X. Fang, J. Jiang, M. Zhang, Revisiting thermodynamic topologies of black holes. JHEP **2301**, 102 (2023)
21. C. Fairoos, T. Sharqui, Topological nature of black hole solutions in dRGT massive gravity. arXiv:2304.02889 [gr-qc]
22. T.N. Hung, C.H. Nam, Topology in thermodynamics of regular black strings with Kaluza–Klein reduction. Eur. Phys. J. C **83**, 582 (2023)
23. Y.Z. Du, H.F. Li, Y.B. Ma, Q. Gu, Topology and phase transition for EPYM AdS black hole in thermal potential. arXiv:2309.00224 [hep-th]
24. M.Y. Zhang, H. Chen, H. Hassanabadi, Z.W. Long, H. Yang, Topology of nonlinearly charged black hole chemistry via massive gravity. Eur. Phys. J. C **83**, 773 (2023)
25. R. Li, C.H. Liu, K. Zhang, J. Wang, Topology of the landscape and dominant kinetic path for the thermodynamic phase transition of the charged Gauss–Bonnet AdS black holes. Phys. Rev. D **107**, 044003 (2023)
26. M. Rizwan, K. Jusufi, Topological classes of thermodynamics of black holes in perfect fluid dark matter background. Eur. Phys. J. C **83**, 944 (2023)
27. M.U. Shahzad, A. Mehmood, S. Sharif, A. Övgün, Topological classes of thermodynamics of black holes in perfect fluid dark matter background. Eur. Phys. J. C **83**, 944 (2023)
28. C.W. Tong, B.H. Wang, J.R. Sun, Topology of black hole thermodynamics via Renyi statistics. arXiv:2310.09602 [gr-qc]
29. M.R. Alipour, M.A.S. Afshar, S.N. Gashti, J. Sadeghi, Topological classification and black hole thermodynamics. Phys. Dark Universe **42**, 101361 (2023)
30. N.J. Gogoi, P. Phukon, Topology of thermodynamics in R-charged black holes. Phys. Rev. D **107**, 106009 (2023)
31. N.J. Gogoi, P. Phukon, Thermodynamic topology of 4D Dyonic AdS black holes in different ensembles. Phys. Rev. D **108**, 066016 (2023)
32. J. Sadeghi, S. Noori Gashti, M.R. Alipour, M.A.S. Afshar, Bardeen black hole thermodynamics from topological perspective. Ann. Phys. **455**, 169391 (2023)
33. M.Y. Zhang, H. Chen, H. Hassanabadi, Z.W. Long, H. Yang, Topology of nonlinearly charged black hole chemistry via massive gravity. Eur. Phys. J. C **83**, 773 (2023)
34. D.Y. Chen, Y.C. He, J. Tao, Topology of higher-dimensional black holes' thermodynamics in massive gravity. Eur. Phys. J. C **83**, 872 (2023)
35. M.S. Ali, H. El Moumni, J. Khalloufi, K. Masmar, Topology of Born–Infeld-AdS black hole phase transition. arXiv:2306.11212 [hep-th]
36. P.V.P. Cunha, C.A.R. Herdeiro, Stationary black holes and light rings. Phys. Rev. Lett. **124**, 181101 (2020)
37. M. Guo, S. Gao, Universal properties of light rings for stationary axisymmetric spacetimes. Phys. Rev. D **103**, 104031 (2021)
38. H.C.D.L. Junior, J.Z. Yang, L.C.B. Crispino, P.V.P. Cunha, C.A.R. Herdeiro, Einstein–Maxwell-dilaton neutral black holes in strong magnetic fields: topological charge, shadows and lensing. Phys. Rev. D **105**, 064070 (2022)
39. S.W. Wei, Y.X. Liu, R.B. Mann, Intrinsic curvature and topology of shadows in Kerr spacetime. Phys. Rev. D **99**, 041303(R) (2019)
40. S.W. Wei, Topological charge and black hole photon spheres. Phys. Rev. D **102**, 064039 (2020)
41. S.W. Wei, Y.X. Liu, Topology of black hole thermodynamics. Phys. Rev. D **105**, 104003 (2022)
42. S.W. Wei, Y.X. Liu, Topology of equatorial timelike circular orbits around stationary black holes. Phys. Rev. D **107**, 064006 (2023)
43. X. Ye, S.W. Wei, Distinct topological configurations of equatorial timelike circular orbit for spherically symmetric (hairy) black holes. JCAP **07**, 049 (2023)
44. P. Hořava, Quantum gravity at a Lifshitz point. Phys. Rev. D **79**, 084008 (2009)
45. P. Hořava, Membranes at quantum criticality. JHEP **0903**, 020 (2009)
46. P. Hořava, Spectral dimension of the universe in quantum gravity at a Lifshitz point. Phys. Rev. Lett. **102**, 161301 (2009)

47. H. Lü, J. Mei, C.N. Pope, Solutions to Horava gravity. Phys. Rev. Lett. **102**, 091301 (2009)

48. R.G. Cai, L.M. Cao, N. Ohta, Topological black holes in Horava–Lifshitz gravity. Phys. Rev. D **80**, 024003 (2009)

49. R.G. Cai, L.M. Cao, N. Ohta, Thermodynamics of black holes in Horava–Lifshitz gravity. Phys. Lett. B **679**, 504 (2009)

50. Q.J. Cao, Y.X. Chen, K.N. Shao, Black hole phase transitions in Horava–Lifshitz gravity. Phys. Rev. D **83**, 064015 (2011)

51. R.G. Cai, Y. Liu, Y.W. Sun, On the z = 4 Horava–Lifshitz gravity. JHEP **0906**, 010 (2009)

52. M.B. Jahani Poshteh, R.B. Mann, Thermodynamics of z = 4 Horava–Lifshitz black holes. Phys. Rev. D **103**, 104024 (2021)

53. D.Y. Chen, H.T. Yang, X.T. Zu, Hawking radiation of black holes in the z = 4 Horava–Lifshitz gravity. Phys. Lett. B **681**, 463 (2009)